

Predicting the dynamics of ground settlement and its derivatives caused by tunnelling in soil

by P. B. ATTEWELL*, DEng, PhD, MICE, & J. P. WOODMAN*, MSc

Equations are developed for the prediction of the three-dimensional ground movements and strains caused by tunnelling in soil. Predicted settlements are compared with some reported case histories and a worked example for the calculation of deformations and strains is given.

1. Introduction

AT THE PLANNING STAGE of a tunnelling scheme, and in the light of factual and interpretive ground investigation evidence, the project promoter or his representative will be keen to ensure, by choice of appropriate construction techniques and aids, that structures adjacent to the tunnel suffer no damage or disruption as a result of the tunnelling operations. Any attempt to predict the effects of ground movements, caused by excavation, on buildings and in-ground structures such as water and gas mains encounters difficulties not only of a theoretical nature but also arising from the requirement to have sufficient information about practical circumstances. However, recognition of these problems does not significantly reduce the need for predictive information on induced movements in the soil. The analyses outlined in this Paper were developed as a result of particular environmental problems, and it is suggested that any predictions based on the analyses are likely to be more relevant to overall planning and design than to specific practical cases.

During recent years numerous case histories of ground movement measurements have been reported in the literature. Most of the measurements relate to ground surface since it is less easy to instrument for and actually measure movements below ground. Furthermore, the surface measurements are usually restricted to vertical movements, or settlements, since the measurement of lateral movement again pres-

ents some difficulty. But a more severe limitation arises with respect to the data interpretation. Measured movements ahead of the tunnel face have effectively been ignored in the interpretation, attention having been concentrated on the permanent set movements that have developed in planes transverse (normal) to the tunnel centre-line and behind the face. However, above-ground and in-ground structures will respond transiently to the forward (of the tunnel face) elements of the settlement trough, and before any more complex structural analysis can be contemplated it is necessary to provide an interpretive three-dimensional setting for the expected ground movements.

A useful starting point for the analysis is the form of the transverse settlement trough that has developed after passage of the tunnel face. It is assumed that most of the displaced volume of the trough per unit distance of face advance can be attributed to face- and radial-take losses. These have been discussed in some detail by Attewell (1978). As time passes, and the face advances well beyond the transverse vertical plane of interest, additional time-dependent settlements caused by such mechanisms as ground consolidation are superimposed on the ground-loss settlements. These longer-term processes of special importance in clay soils, and which will increase the final volume of the surface settlement depression, contribute relatively little to the early transient de-

formation picture, and so are not considered in the Paper.

There seems to be reasonable case history evidence from tunnelling in different generally-cohesive soils ranging from clays (see, for example, Schmidt, 1969; Peck, 1969; Attewell & Farmer, 1974; Attewell *et al.*, 1978; Glossop & Farmer, 1977; Glossop, 1980) to fill (Dobson *et al.*, 1979; McDermott, 1979) that the permanent transverse settlement profile can be described in terms of a normal probability, or Gaussian, equation (Fig. 1). The application of such an equation to settlement troughs in granular soils is less secure. For the more cohesive soils the method of measurement data fits to a normal probability equation has been noted in Attewell (1978) and Dobson *et al.* (1979), and it is found—as might be expected—that the quality of fit is variable. In spite of attempts to formulate other functions for particular cases it has been concluded that the normal probability curve remains the most appropriate for fitting to transverse settlement profiles in general, and for use in the prediction of permanent settlement distribution (Norgrove *et al.*, 1979). Stochastic analysis also provides analytical justification for its adoption (Litwiniszyn, 1956; Sweet & Bogdanoff, 1965; Glossop, 1977; Attewell, 1978). Having achieved a best-fit curve to transverse settlement data, the particular profile may then be characterised by its maximum settlement (equivalent to the mean point of a statis-

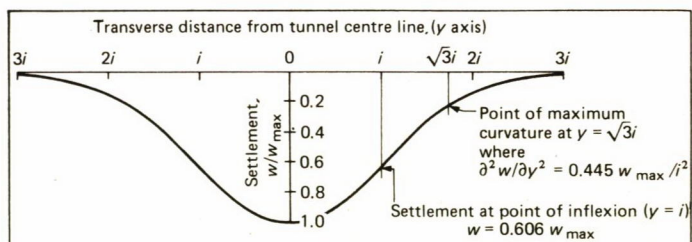


Fig. 1. Normal probability form of transverse settlement profile

*Engineering Geology Laboratories, University of Durham, England

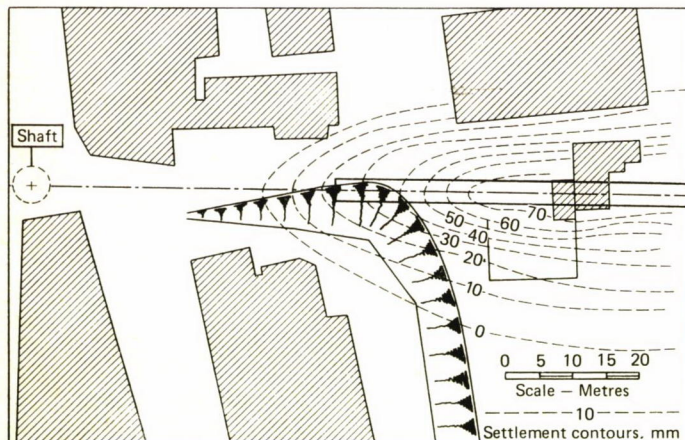


Fig. 2(a). Measured distribution of ground settlement above a tunnel (face entered clay; upper overburden fill)

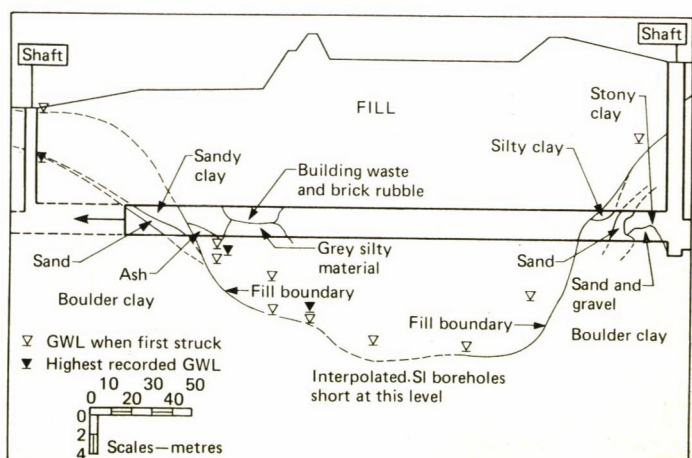


Fig. 2(b). Cross-section of tunnel for Fig. 2(a)

tical normal distribution), and the transverse distance from that maximum to the point of inflexion or maximum gradient (equivalent to the standard deviation of a statistical normal distribution). These two parameters, classified with respect to the type of ground and tunnel geometry (excavated face area and depth below ground surface), may then be used for the prediction of settlement and settlement derivatives (displacement, strain, gradient, curvature) across the transverse profile (Norgrove *et al.*, 1979).

Having accepted the normal probability curve in respect of the transverse settlement trough, it seems logical to assign a cumulative probability function to the settlement trough on the tunnel centre line projecting forward from the face, noting the general form of settlement distribution about a tunnel face as typified in Fig. 2. The aim of this present Paper is to investigate such a procedure by analysis and by reference to some case history data, and also to derive equations for settlement, lateral displacement, and strain, that might be used predictively for any point on the ground surface radially distant from the tunnel face.

It is emphasised that the present Paper is concerned largely with predicted ground deformation parameters. The amplitudes and amplitude-locations of each parameter should not be interpreted directly in terms of structural deformations. It is of interest to note that Geddes (1978, 1981) has suggested one method of approaching the ground-structure interaction problem in the context of coal mining subsidence.

2. Analysis

Fig. 3 shows the coordinate system to be adopted: x , or x_1 —parallel to the tunnel centre line; y , or x_2 —transverse (normal) to the tunnel centre line; z , or x_3 —vertical. The respective displacements and strains are u , v , w , ϵ_x , ϵ_y , ϵ_z . Thus, the settlement in this notation is w rather than s or δv , which have been used previously in the literature. The tunnel is at depth z_0 .

In conformity with earlier Papers (see, for example, Norgrove *et al.*, 1979, Appendix 2), the following symbols apply:

V is the volume (m^3) displaced by the settlement per unit face advance (m) for a linear loss source, and is simply the volume displaced for a point loss source;

i is the transverse horizontal distance between the points of maximum settlement and inflexion at depth z given by $i = K_a \left\{ \frac{z_0 - z}{2a} \right\}^n$, where

n is usually an empirical parameter but may sometimes be derived theoretically,

a is a material parameter, and

K_a is chosen in accordance with the definition of a .

A discussion on the justification of equations of this type is given in Attewell (1978), and in Appendix A.

2.1 Point source of loss

Consider, first, a point source of ground loss at $x_0 = 0$, $y_0 = 0$, z_0 . Let r be the horizontal radial coordinate ($= \sqrt{x^2 + y^2}$), and let p be the radial displacement ($p = 0$ when $x = y = r = 0$). The tangential displacement q equals 0 as a consequence of circular symmetry.

Then, on the basis of experimental evidence or stochastic theory, the following

assumption is made for ground that is flat or nearly flat relative to source depth:

$$w = \frac{V}{2\pi i^2} \exp \left[\frac{-r^2}{2i^2} \right], \quad z < z_0 \dots (1),$$

$$\text{and so, given that } \frac{i}{a} = K_a \left\{ \frac{z_0 - z}{2a} \right\}^n,$$

$$\epsilon_z = \frac{\partial w}{\partial z} = -w \left(\frac{r^2}{i^2} - 2 \right) \frac{n}{z_0 - z} \dots (2).$$

For non-flat ground this assumption can also be made, but only at levels below those of neighbouring ground troughs, or at least close to them in comparison with source depth.

It is further assumed that the soil at ground surface undergoes no volumetric strain as settlement develops, that is,

$$\epsilon_r + \epsilon_\theta + \epsilon_z = 0 \dots (3),$$

with ϵ_θ written as the hoop strain. The above equality is clearly approximate and arguable, but under the envisaged conditions of low confinement it is thought to be not unreasonable.

Since

$$\epsilon_r = \frac{\partial p}{\partial r} \dots (4),$$

and

$$\epsilon_\theta = -\frac{1}{r} \frac{\partial q}{\partial \theta} = -\frac{p}{r} \quad (\text{because } q=0) \dots (5),$$

then

$$\begin{aligned} \epsilon_r + \epsilon_\theta &= \frac{\partial p}{\partial r} + \frac{p}{r} = -\epsilon_z \\ &= \frac{n}{z_0 - z} w \left(\frac{r^2}{i^2} - 2 \right) \dots (6). \end{aligned}$$

The solution of eqn. 6 with boundary condition $p = 0$ at $r = 0$ is given by

$$\begin{aligned} p &= \frac{1}{r} \int_0^r \frac{n}{z_0 - z} \frac{V}{2\pi i^2} \left(\frac{r'^3}{i^2} - 2r' \right) \times \\ &\quad \exp \left[\frac{-r'^2}{2i^2} \right] dr' \\ &= \frac{-n}{z_0 - z} rw \dots (7). \end{aligned}$$

Now

$$u = \frac{x}{r} p \dots (8),$$

and

$$v = \frac{y}{r} p \dots (9),$$

therefore

$$u = \frac{-n}{z_0 - z} xw \dots (10),$$

and

$$v = \frac{-n}{z_0 - z} yw \dots (11).$$

It follows that

$$\epsilon_x = \frac{\partial u}{\partial x} = \frac{n}{z_0 - z} w \left(\frac{x^2}{i^2} - 1 \right) \dots (12),$$

and

$$\epsilon_y = \frac{\partial v}{\partial y} = \frac{n}{z_0 - z} w \left(\frac{y^2}{i^2} - 1 \right) \dots (13).$$

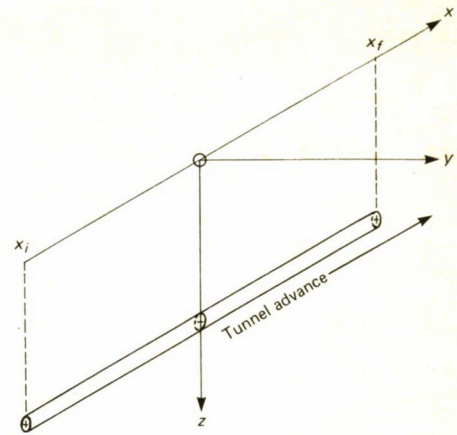


Fig. 3. Tunnel coordinate system

2.2 Linear source of loss

The foregoing equations are of limited value to the practical tunnelling case. It is necessary to consider a point source of loss at depth z_0 , on the line $y = 0$, moving forwards along the x -coordinate axis from x_i to x_f . (Subscript ' i ' is used to denote 'initial' or tunnel start point, and subscript ' f ' denotes 'face' or 'final'). The condition is shown in Fig. 3. Time will be subsumed under the parameter x_f , and so it will not be taken into account specifically. In effect this means that the rate of tunnel advance is assumed to be slow compared to the dynamics of ground movement, or that tunnel advance has stopped temporarily at x_f , and time is allowed for dynamic effects to fade away before measurements of ground movement are taken. By using an effective value of x_f one may approximate the situation when radial loss occurs over a short length of tunnel as well as face loss, or when the tunnel moves at a moderate but constant speed.

It is supposed that ground loss settlements consequent to increments of tunnel advance are additive. In this case

$$\begin{aligned} w &= \frac{V}{2\pi i^2} \int_{x_i}^{x_f} \exp \left[\frac{-(x-x_0)^2 + y^2}{2i^2} \right] dx_0 \\ &= \frac{V}{\sqrt{2\pi i^2}} \exp \left[\frac{-y^2}{2i^2} \right] \left\{ G \left(\frac{x-x_i}{i} \right) \right. \\ &\quad \left. - G \left(\frac{x-x_f}{i} \right) \right\} \dots (14), \end{aligned}$$

where

$$G(x) = \frac{1}{\sqrt{2\pi}} \int_{-\infty}^x \exp \left[\frac{-\beta^2}{2} \right] d\beta \dots (15)$$

can be found from standard probability tables (see Table I). In particular,

$$G(0) = \frac{1}{2},$$

and

$$G(\infty) = 1.$$

In practice, given that the tunnel is sufficiently deep to be regarded as a linear source, then the prediction of settlement using eqn. 14 may be resolved into the following steps:

- Estimate the volume ground loss V per unit distance of advance. Do this by mea-

surement on a transverse profile — on-site levelling when the tunnel face has advanced a distance of approximately z_0 beyond the measurement line, followed by scale section planimeter integration or by the use of the equation $V = \sqrt{2\pi} i w_{\max}$ — or from a consensus of case history evidence of tunnelling in similar soils (see Attewell, 1978). The existence of consolidation will complicate this calculation, but there are two approaches under which the use of eqn. 14 is acceptable. The consolidation component of a composite ground loss-consolidation V may be extracted in order to predict the corresponding consolidation-free component of settlement. Alternatively, it may be retained if consolidation does not alter the source distribution in such a way as to significantly change the form of w .

(b) Estimate the transverse profile inflection distance i . (Again, do this by direct measurement on a fully-established transverse profile, or from a consensus of case history evidence).

(c) Note the y (tranverse) coordinate distance from the tunnel centre line for the point of interest on ground surface.

(d) Take the differences between the x -coordinate of this point and the x -coordinates of starting (x_i) and current (x_f) points, with the proviso that x_f may have to be replaced by an effective value — see later discussion. Normalise each of the two values by i , and determine in each case the cumulative probability from Table I.

To illustrate the procedure, consider the following example, which relates to the Fig. 4 case history:

$$w_{\max} = 7.86 \text{ mm}; i = 3.9 \text{ m.}$$

$$\text{Thus, } V = 0.08 \text{ m}^3/\text{m.}$$

$$\text{Let } (x - x_f) = 4 \text{ m}; (x - x_i) \rightarrow \infty; y = 1.5 \text{ m.}$$

$$\text{Therefore, } G\left(\frac{x - x_i}{i}\right) = 1; G\left(\frac{x - x_f}{i}\right)$$

$$= G(1.02) = 0.846 \text{ (from Table I).}$$

It follows that $w = 1.12 \text{ mm.}$

Eqn. 14 can be expressed in the form

$$w = w_{\infty} \left\{ G\left(\frac{x - x_i}{i}\right) - G\left(\frac{x - x_f}{i}\right) \right\} \quad \dots (16),$$

where

$$w_{\infty} = \frac{V}{\sqrt{2\pi} i} \exp\left[\frac{-y^2}{2i^2}\right] \quad \dots (17)$$

is the asymptotic form of w as $x_i \rightarrow -\infty$, $x_f \rightarrow \infty$. w_{∞} is the established 2-dimensional 'permanent set' normal probability settlement form used by the several authors quoted above.

Assuming that $\frac{i}{a} = K_a \left\{ \frac{z_0 - z}{2a} \right\}$, other results follow from eqn. 14. For the vertical strain:

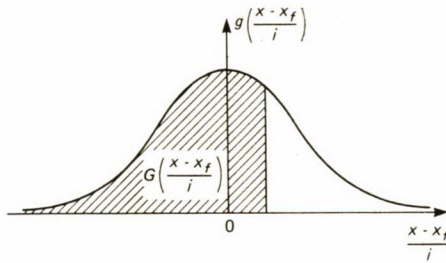
$$\epsilon_z = \frac{\partial w}{\partial z} = \frac{-n}{z_0 - z} w_{\infty} \left\{ \frac{-1}{\sqrt{2\pi}} \left\{ \left(\frac{x - x_i}{i}\right) \times \right. \right. \dots$$

$$\left. \left. \exp\left[\frac{-(x - x_i)^2}{2i^2}\right] - \left(\frac{x - x_f}{i}\right) \times \right. \right. \dots$$

TABLE I. NUMERICAL INTEGRATION OF THE NORMAL PROBABILITY CURVE

Table of $G\left(\frac{x - x_f}{i}\right)$

$(x - x_f)/i$	0	1	2	3	4	5	6	7	8	9
0.0	.500	.504	.508	.512	.516	.520	.524	.528	.532	.536
0.1	.540	.544	.548	.552	.556	.560	.564	.567	.571	.575
0.2	.579	.583	.587	.591	.595	.599	.603	.606	.610	.614
0.3	.618	.622	.626	.629	.633	.637	.641	.644	.648	.652
0.4	.655	.659	.663	.666	.670	.674	.677	.681	.684	.688
0.5	.691	.695	.698	.702	.705	.709	.712	.716	.719	.722
0.6	.726	.729	.732	.736	.739	.742	.745	.749	.752	.755
0.7	.758	.761	.764	.767	.770	.773	.776	.779	.782	.785
0.8	.788	.791	.794	.797	.800	.802	.805	.808	.811	.813
0.9	.816	.819	.821	.824	.826	.829	.831	.834	.836	.839
1.0	.841	.844	.846	.848	.851	.853	.855	.858	.860	.862
1.1	.864	.867	.869	.871	.873	.875	.877	.879	.881	.883
1.2	.885	.887	.889	.891	.893	.894	.896	.898	.900	.901
1.3	.903	.905	.907	.908	.910	.911	.913	.915	.916	.918
1.4	.919	.921	.922	.924	.925	.926	.928	.929	.931	.932
1.5	.933	.934	.936	.937	.938	.939	.941	.942	.943	.944
1.6	.945	.946	.947	.948	.949	.951	.952	.953	.954	.954
1.7	.955	.956	.957	.958	.959	.960	.961	.962	.962	.963
1.8	.964	.965	.966	.966	.967	.968	.969	.969	.970	.971
1.9	.971	.972	.973	.973	.974	.974	.975	.976	.976	.977
2.0	.977	.978	.978	.979	.979	.980	.980	.981	.981	.982
2.1	.982	.983	.983	.983	.984	.984	.985	.985	.985	.986
2.2	.986	.986	.987	.987	.987	.988	.988	.988	.989	.989
2.3	.989	.990	.990	.990	.990	.991	.991	.991	.991	.992
2.4	.992	.992	.992	.992	.993	.993	.993	.993	.993	.994
2.5	.994	.994	.994	.994	.994	.995	.995	.995	.995	.995
2.6	.995	.995	.996	.996	.996	.996	.996	.996	.996	.996
2.7	.997	.997	.997	.997	.997	.997	.997	.997	.997	.997
2.8	.997	.998	.998	.998	.998	.998	.998	.998	.998	.998
2.9	.998	.998	.998	.998	.998	.998	.998	.999	.999	.999
3.0	.999	.999	.999	.999	.999	.999	.999	.999	.999	.999



$$\exp\left[-\frac{(x - x_f)^2}{2i^2}\right] + \left(\frac{y^2}{i^2} - 1\right) \times \left[G\left(\frac{x - x_i}{i}\right) - G\left(\frac{x - x_f}{i}\right) \right] \dots (18).$$

The transverse, y -coordinate displacement is given by

$$v = \frac{-n}{z_0 - z} yw \quad \dots (19),$$

where w is given by eqn. 14.

The y -coordinate strain is

$$\epsilon_y = \frac{\partial v}{\partial y} = \frac{n}{z_0 - z} w \left(\frac{y^2}{i^2} - 1 \right) \dots (20).$$

The x -coordinate displacement is given by

$$u = \frac{-n}{z_0 - z} \frac{V}{2\pi i^2} \int_{x_i}^{x_f} (x - x_0) \times \exp\left[-\frac{(x - x_0)^2 + y^2}{2i^2}\right] dx_0 \dots (21).$$

$$= \frac{n}{z_0 - z} w_{\infty} \frac{i}{\sqrt{2\pi}} \left\{ \exp\left[-\frac{(x - x_i)^2}{2i^2}\right] - \exp\left[-\frac{(x - x_f)^2}{2i^2}\right] \right\} \dots (22).$$

The x -coordinate strain is

$$\epsilon_x = \frac{\partial u}{\partial x} = \frac{-n}{z_0 - z} w_{\infty} \frac{1}{\sqrt{2\pi}} \left\{ \left(\frac{x - x_i}{i}\right) \times \right. \dots (23).$$

$$\exp\left[-\frac{(x - x_i)^2}{2i^2}\right] - \left(\frac{x - x_f}{i}\right) \times \exp\left[-\frac{(x - x_f)^2}{2i^2}\right] \dots (24).$$

Since ground gradient has been used as one criterion for predicting the stability of a surface building (Norgrove *et al.*, 1979), and since it can also affect the integrity of, say, a linear in-ground structure such as a pipe, it is useful to obtain an expression for that gradient θ .

Along the y -coordinate axis

$$\theta_y \simeq \frac{\partial w}{\partial y} = \frac{-y}{i^2} w = \frac{\partial w_{\infty}}{\partial y} \left\{ G\left(\frac{x - x_i}{i}\right) - G\left(\frac{x - x_f}{i}\right) \right\} \dots (25).$$

and along the x -coordinate axis

$$\theta_x \simeq \frac{\partial w}{\partial x} = \frac{w_{\infty}}{\sqrt{2\pi} i} \left\{ \exp\left[-\frac{(x - x_i)^2}{2i^2}\right] - \exp\left[-\frac{(x - x_f)^2}{2i^2}\right] \right\} \dots (26).$$

where x' ($=x+u$) and y' ($=y+v$) are the final position coordinates.

Excavations of finite width and length at depth z_0 are immediate generalisations of the above results. In particular, the vertical displacement is still given by eqn. 16, but

$$\text{with } w_\infty = V \left\{ G \left(\frac{y-y_i}{i} \right) - G \left(\frac{y-y_f}{i} \right) \right\}$$

and V defined as the volume displaced per unit areal face advance. Excavations of finite volume are best treated by noting that ground loss only occurs at the boundary surface of the excavation, but there is another complication. The existence of a finite hole violates the assumption of material continuity, so that, even within the framework of this particular theory, results are approximate only, unless this specific problem is treated.

2.3 Structural deformation

When considering the integrity of a grounded structure, the direct connection of the above results to structural displacement and strains is problematic. Indeed, this is true for any theoretical approach that does not specifically include the geometry, and the material constitutive relations of the structure itself. Accordingly, the remaining displacement derivatives are included in Appendix B. If ground integrity is of interest, or in the unlikely event that structure and ground are indistinguishable in terms of material behaviour (except possibly in failure point), the shear strains and rotations are given in terms of the derivatives by the following formulae:

$$\gamma_{ij} = \frac{\partial u_j}{\partial x_i} + \frac{\partial u_i}{\partial x_j} \quad \dots (25)$$

$$\omega_k = \frac{1}{2} \left(\frac{\partial u_j}{\partial x_i} - \frac{\partial u_i}{\partial x_j} \right) \quad \dots (26)$$

Note that $\omega_z = 0$ for both linear and point sources, since $\frac{\partial v}{\partial x} = \frac{\partial u}{\partial y}$.

Given that, at the levels in the ground of structural significance, the assumption $\varepsilon_x + \varepsilon_y + \varepsilon_z = 0$ is reasonable, the results in this Paper can be used as boundary conditions for conventional stress analysis of grounded structures. However, there is one other proviso. Under the aegis of stochastic theory used in the calculation of w , basic assumptions are violated by the structure. Although it may conceivably satisfy the same material constitutive relations as the ground, it cannot respond in the same way to random displacements (almost by definition). This will always have a local effect, but if the structure is sufficiently extensive the global volume loss may also be influenced to produce large errors (large variations in ground surface produce similar results). The empirical approach to the form of w does not explicitly, or implicitly, make the assumptions underlying stochastic theory, but it is likely that experimental observation would demonstrate analogous effects. This point will not be considered further. It will also be assumed that material non-linear behaviour can be catered for.

Once slipping occurs at the ground-structure interface, displacement rather than strain becomes the material constitutive parameter over areas of slippage

(Geddes, 1978, 1981). It is sometimes appropriate to resolve the slip displacement function on the interface into a mean translation, and a differential displacement function. If the structure is small, a Taylor series approximation to the displacement function may be adequate, but although strain reappears as a parameter its use is fundamentally different from that before slipping.

By way of example, two contrasting and limiting cases follow. In the first place, consider a pipe, which is materially indistinguishable from the ground, buried parallel to the x -axis. Competence of the pipe can be assessed in terms of the ground strain components, but it is more useful to consider parameters that are more appropriate to the pipe geometry. Assuming that the pipe is not subject to crushing or shear failure, then, under conditions of small strain, the most important parameters are

axial strain, ε_x ,

$$\text{the material curvatures, } \frac{-\partial \omega_y}{\partial x}, \text{ and } \frac{\partial \omega_z}{\partial x},$$

$$\text{and the torsional strain, } \frac{\partial \omega_x}{\partial x}.$$

The general case also requires ε_y , ε_z , γ_{xy} , γ_{yz} and γ_{zx} .

Now suppose that the same pipe is furnished with an almost perfectly smooth surface such that the small frictional force generated on the surface is proportional to slip. There will be a loss of shear across the ground-pipe interface but, for simplicity, the effect on the displacement field will be neglected. Let \bar{u} be the mean ground displacement along the line of the pipe. (If there are external constraints on the axial movement of the pipe, then put $\bar{u} = 0$). Then the displacement field in the pipe (structure S) is given approximately by

$$u_s \approx \bar{u} \\ v_s \approx v(x, y_s, z_s) \\ w_s \approx w(x, y_s, v_s) \quad \dots (27)$$

where x is the apparent initial position of the point at x_s relative to the ground. x is found by equating position coordinates after displacement, in ground, and S .

$$x' = X(x) = x + u(x) = x_s + \bar{u} \quad \dots (28)$$

Therefore,

$$x \approx X^{-1}(x_s + \bar{u}) \quad \dots (29)$$

Alternatively, from eqn. 28

$$x_s + \bar{u} \approx x + u(x_s) + \frac{\partial u}{\partial x} \Big|_{x_s} (x - x_s) \quad \dots (30)$$

Therefore,

$$x \approx x_s + \frac{\bar{u} - u(x_s)}{1 + \frac{\partial u}{\partial x}} \Big|_{x_s} \quad \dots (31)$$

$$\approx x_s + \bar{u} - u(x_s) \quad \dots (32)$$

if $\frac{\partial u}{\partial x} \Big|_{x_s} (x - x_s)$ is small (small strain)

and/or small slip, $x - x_s \approx \bar{u} - u(x_s)$. From eqn. 27,

$$v_s \approx v(x, y_s, z_s) \\ \approx v(x_s, y_s, z_s) + \frac{\partial v}{\partial x} \Big|_{x_s} (\bar{u} - u(x_s)) \quad \dots (33)$$

$$\approx v(x_s, y_s, z_s) \text{ for small strain and/} \\ \text{or slip} \quad \dots (34)$$

Similar arguments apply for w_s .

The axial strain $\varepsilon_{x_s} = \frac{\partial u_s}{\partial x_s} = 0$, and there is no shear or torsional strain either.

The parameters that remain are $\frac{\partial^2 w_s}{\partial x_s^2}$,

$$\text{and } \frac{\partial^2 v_s}{\partial x_s^2}.$$

Another common structure is a horizontal planar slab foundation perpendicular to the z -axis. If it follows ground displacement exactly, the relevant parameter

$$\text{list is } \varepsilon_x, \varepsilon_y, \gamma_{xy}, \frac{-\partial \omega_y}{\partial x}, \frac{\partial \omega_x}{\partial y}, \frac{\partial \omega_x}{\partial x} \approx -\frac{\partial \omega_y}{\partial y}.$$

Parameters ε_z , γ_{yz} , γ_{zx} may be ad-

ded if needed. When the slab is almost perfectly smooth, only the bending terms $\frac{\partial^2 w_s}{\partial x_s^2}$, $\frac{\partial^2 w_s}{\partial y_s^2}$, and $\frac{\partial^2 w_s}{\partial x_s \partial y_s}$, are re-

quired, and the calculation of u_s , v_s , w_s is analogous to that for the smooth pipe.

By paying excessive attention to the detailed analysis, and in regarding the above examples simply as limiting cases, there is a risk of ignoring what could turn out to be good first-order approximations in many cases. Whenever the stress-bearing part of the structure is sufficiently thin, on strain-energy considerations the total force it can exert is relatively small whatever its stiffness, ground-structure interaction will be highly localised, and provided that the ground does not shear and flow normally to the structure by this interaction then structural displacement will be close to ground displacement. In this situation, the 'rough' and 'smooth' models may be considered reasonable approximations to structures with and without protuberances (flanges, for example, in the case of in-ground pipes), respectively.

2.4 Stationary points on the linear-source displacement profile

There are obvious difficulties of accurately relating structural movement to ground movement. One method of tackling the problem would be to create a 3-D finite element model of the structure in-ground, to apply the theoretical ground displacements u , v , w to the boundaries of the soil-structure system, and to observe the induced strains in the structure. Since the location of any structural failures will be determined by the position of certain maxima on the displacement profile, and since the values of these maxima could be helpful in assessing the risk of failure, it is

reasonable also to examine the analytical expressions for the maxima and their locations.

Let G' denote the factor $G\left(\frac{x-x_i}{i}\right) - G\left(\frac{x-x_f}{i}\right)$, which becomes $1 - G\left(\frac{x-x_f}{i}\right)$

as $x_i \rightarrow -\infty$ for a semi-infinite tunnel. On transverse profiles, x is constant, and the following equations are obtained simply by inspection or differentiation of earlier results:

$$w_{\max} = \frac{V}{\sqrt{2\pi} i} G' \text{ at } y = 0 \quad \dots (35).$$

$$|v|_{\max} = \frac{n}{z_0 - z} \frac{V}{\sqrt{2\pi}} \exp\left[-\frac{1}{2}\right] G' \text{ at } y = \pm i \quad \dots (36).$$

$$\epsilon_{y_{\max}} = \frac{-n}{z_0 - z} \frac{V}{\sqrt{2\pi} i} G' \text{ at } y = 0 \quad \dots (37).$$

$$\epsilon_{y_{\text{tmax}}} = \frac{n}{z_0 - z} \frac{V}{\sqrt{2\pi} i} 2 \exp\left[-\frac{3}{2}\right] G' \text{ at } y = \pm \sqrt{3} i \quad \dots (38).$$

$$|\theta_{y'}|_{\max} \approx \frac{V}{\sqrt{2\pi} i^2} \exp\left[-\frac{1}{2}\right] G' \text{ at } y \approx \pm i \quad \dots (39).$$

By eqn. 23

$$\frac{\partial^2 w}{\partial y^2} = \frac{w}{i^2} \left(\frac{y^2}{i^2} - 1 \right) \quad \dots (40).$$

Hence, maximum bending in the vertical plane of a horizontal transverse pipe is

$$\frac{2V}{\sqrt{2\pi} i^3} \exp\left[-\frac{3}{2}\right] G', \text{ and occurs at}$$

$y = \pm \sqrt{3} i$. Maximum bending in the horizontal plane also occurs at $y = \pm \sqrt{3} i$, and has the value

$$\frac{-n}{z_0 - z} \frac{V}{\pi i^2} \exp\left[-\frac{3}{2}\right] \times \left\{ \exp\left[\frac{-(x-x_i)^2}{2i^2}\right] - \exp\left[\frac{-(x-x_f)^2}{2i^2}\right] \right\}.$$

Most of these equations replicate the earlier-published equations for the transverse trough case except for the multiplying factor G' .

For the off-centre line profile y is constant, and a related set of results can be obtained. Let x_m denote the mid-point x -coordinate of the tunnel, and $2l = x_f - x_i$, tunnel length. Arrows ' \rightarrow ' are used to indicate limiting values for the semi-infinite tunnel when $x_i \rightarrow -\infty$.

$$w_{\max} = w_{\infty} \left\{ 2G\left(\frac{l}{i}\right) - 1 \right\} \text{ at } x = x_m \quad \dots (41),$$

$$\rightarrow w_{\infty} \text{ at } x \rightarrow -\infty \text{ as } x_i \rightarrow -\infty \text{ (any } x \text{ if } x_f \rightarrow \infty \text{ as well)} \quad \dots (42).$$

$$|u|_{\max} = \frac{n}{z_0 - z} w_{\infty} \frac{i}{\sqrt{2\pi}} \frac{2l}{s+l} \times \exp\left[\frac{-(s-l)^2}{2i^2}\right] \text{ at } x = x_m \pm s \quad \dots (43),$$

$$\rightarrow \frac{n}{z_0 - z} w_{\infty} \frac{i}{\sqrt{2\pi}} \text{ at } x = x_f \quad \dots (44),$$

where s is the positive root of

$$(s+l) \exp\left[\frac{-(s+l)^2}{2i^2}\right] = (s-l) \times \exp\left[\frac{-(s-l)^2}{2i^2}\right] \quad \dots (45).$$

This equation also gives an approximation to the stationary points of $\theta_{x'}$.

$$|\theta_{x'}|_{\max} \approx \left| \frac{\partial w}{\partial x} \right|_{\max} = \frac{w_{\infty}}{\sqrt{2\pi} i} \frac{2l}{s+l} \times$$

$$\exp\left[\frac{-(s-l)^2}{2i^2}\right] \quad \dots (46),$$

$$\rightarrow \frac{w_{\infty}}{\sqrt{2\pi} i} \quad \dots (47).$$

$$\epsilon_{x_{\text{stn}}} = \frac{n}{z_0 - z} \frac{w_{\infty}}{\sqrt{2\pi}} \frac{i}{l} \frac{(t+l)(t-l)+i^2}{(t+l)^2-i^2} \times$$

$$\exp\left[\frac{-(t-l)^2}{2i^2}\right] \text{ at } x = x_m \pm t \quad \dots (48),$$

$$\rightarrow \frac{\pm n}{z_0 - z} \frac{w_{\infty}}{\sqrt{2\pi}} \exp\left[-\frac{1}{2}\right] \text{ at } x = x_f \pm i \quad \dots (49),$$

where t is a positive or zero root of

$$\begin{aligned} & \left\{ (t+l)^2 - i^2 \right\} \exp\left[\frac{-(t+l)^2}{2i^2}\right] \\ &= \left\{ (t-l)^2 - i^2 \right\} \exp\left[\frac{-(t-l)^2}{2i^2}\right] \quad \dots (50). \end{aligned}$$

There are three non-trivial roots $(0, \pm t_1)$ to this equation if $l < \sqrt{3} i$, and five roots $(0, \pm t_1, \pm t_2)$ if $l > \sqrt{3} i$. The solution $t = 0$ yields a compressive maximum or minimum according to whether l is less than or greater than $\sqrt{3} i$, respectively.

$$\epsilon_x|_{x_m} = \frac{-n}{z_0 - z} \frac{w_{\infty}}{\sqrt{2\pi}} \frac{i}{l} \exp\left[-\frac{l^2}{2i^2}\right] \quad \dots (51).$$

Eqn. 50 also locates the following stationary values:

$$\begin{aligned} & \left(\frac{\partial^2 w}{\partial x^2} \right)_{\text{stn}} = \frac{w_{\infty}}{\sqrt{2\pi} i^2} \frac{i(t+l)(t-l)+i^2}{i(t+l)^2-i^2} \times \\ & \quad \exp\left[\frac{-(t-l)^2}{2i^2}\right] \quad \dots (52), \end{aligned}$$

TABLE II. CASE HISTORY TUNNEL AND GROUND INFORMATION

Fig. No.	Tunnel Location	Ground	Excav. dia. $2R$ (m)	Axis depth z_0 (m)	i (m)	K_a	n	Max. settlement w_{\max} (mm)	Trough vol. V (% or m^3/m)	Cohesion c_u (kN/m ²)	Liquid limit (%)	Plastic limit (%)	Bulk density (kN/m ³)	Moisture content m (%)	Permeability k (m/s)
4	N.W.A. Contract 31 Tyneside Sewerage Scheme (Hebburn)	Stony/laminated clay	2.014	7.5	3.9	1	0.98	7.86	0.077m ³ /m	73 to 275	53	23	19.0	28	2×10^{-7}
5	London Transport Jubilee Line (Green Park)	London Clay	4.146	29.3	14.5	-	-	6.1	0.196m ³ /m	266	60 to 90	24 to 30	19.0 to 20.1	23 to 29	-
6	Sewerage tunnel, Sydenham, Belfast	Sleech (soft, saturated alluvial silt) 41 kN/m ² c.a.	2.7	5.75	2.5	-	-	16	2.1%	8.7	84	47	14.8	75	1.57×10^{-7} 3.82×10^{-6}
7	Anglian Water Authority, Haycroft Relief Sewer, Grimsby	Silty clay (Grimsby marine warp) 41 kN/m ² c.a.	3.1	5.7	3.2	-	-	66	16% (1.08m ³ /m without c.a.; 0.65m ³ /m with c.a.)	12	68	27	18.0	50	10^{-10}
8	N.W.A. Contract 276 Tyneside Sewerage Scheme (Ouseburn)	Urban and industrial fill	3.471	13	7.29	1.69	0.69	81	0.355m ³ /m	-	-	-	14.5	21	-
9	Newcastle upon Tyne City Sewer,	Urban fill and stiff dark clay	2.15	11.3	3.5	1	0.8	17.2	0.21m ³ /m	171	35	17	21.0	12	-

$$\rightarrow \frac{\pm w_\infty}{\sqrt{2\pi i^2}} \exp \left[-\frac{1}{2} \right] \dots (53).$$

$$\frac{\partial^2 w}{\partial x^2} \Big|_{x_m} = \frac{-w_\infty}{\sqrt{2\pi i^2}} \frac{i}{i} \exp \left[\frac{-l^2}{2i^2} \right] \dots (54).$$

$$\left(\frac{\partial^2 v}{\partial x^2} \right)_{\text{stn}} = \frac{-n}{z_0 - z} \frac{w_\infty y}{\sqrt{2\pi i^2}} \frac{i}{i} \times \frac{(t+l)(t-l) + i^2}{(t+l)^2 - l^2} \exp \left[\frac{-(t-l)^2}{2i^2} \right] \dots (55),$$

$$\rightarrow \frac{-n}{z_0 - z} \frac{w_\infty y}{\sqrt{2\pi i^2}} \exp \left[-\frac{1}{2} \right] \dots (56).$$

$$\frac{\partial^2 v}{\partial x^2} \Big|_{x_m} = \frac{n}{z_0 - z} \frac{w_\infty y}{\sqrt{2\pi i^2}} \frac{i}{i} \exp \left[\frac{-l^2}{2i^2} \right] \dots (57).$$

3. Case histories: x-coordinate ground settlement

Six settlement case histories are shown in Figs. 4 to 9 inclusive, with some additional data being given in Table II. In most cases they provide some qualified confirmation, via the form of the curves, that the extension of the normal probability curve-fitting concept from the transverse y-axis two-dimensional case to the full three-dimensional profile is reasonable for the important zone of ground movement projecting transiently ahead of the tunnel face. The x-axis offset between the predicted and measured curves arises simply because the 50% w_{\max} point (and the point where the rate of change of settlement maximises) on the former curve has been drawn to coincide with the passage of the tunnel face beneath the point, with the implied assumption that the surface settlement occurs at the same time as the ground loss which causes it. With this last assumption, the separation in each case between the two curves may be taken to indicate that in the case of clay soils a greater percentage of the overall settlement can be attributed to face—and early radial—take as compared with the weaker, less cohesive soils. It is generally understood that a higher percentage of the overall ground loss at a tunnel in more granular soil occurs towards the tail of a shield, and that in such material the total losses are much more dependent on excavation and ground support technique. A suggestion by Craig (1975) as to the partition of the total settlement to the ground loss at a shield-driven tunnel is given below:

Ground	Face of shield	Tail of shield
Sand above water table	30–50%	60–80%
Stiff clays	30–60%	50–75%
Sand below water table	0–25%	50–75%
Silts and soft clays	0–25%	30–50%

Even accepting that some delay on settlement transmission to ground surface must occur (any delay depending, among other factors, upon the type of ground material through which the movements

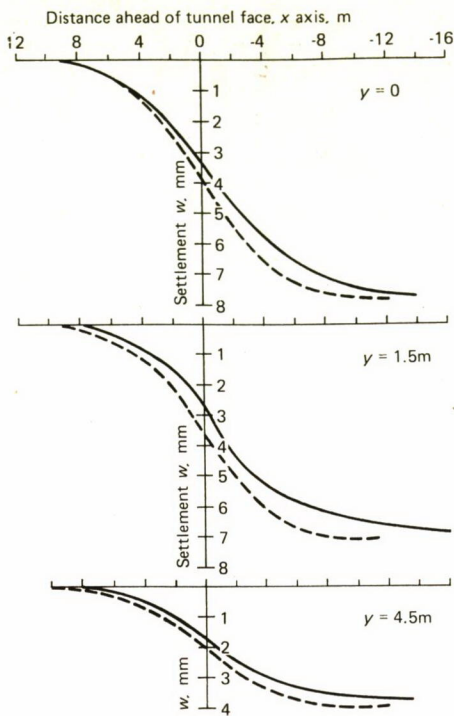


Fig. 4. Forward x-coordinate settlement development profiles for Northumbrian Water Authority's Contract 31 (Hebburn South Bank Interceptor Sewer in stony/laminated clay) (Attewell & Farmer, 1973). Full line is measured profile; broken line is theoretical profile (50% w_{\max} assumed coincident with plane of tunnel face)

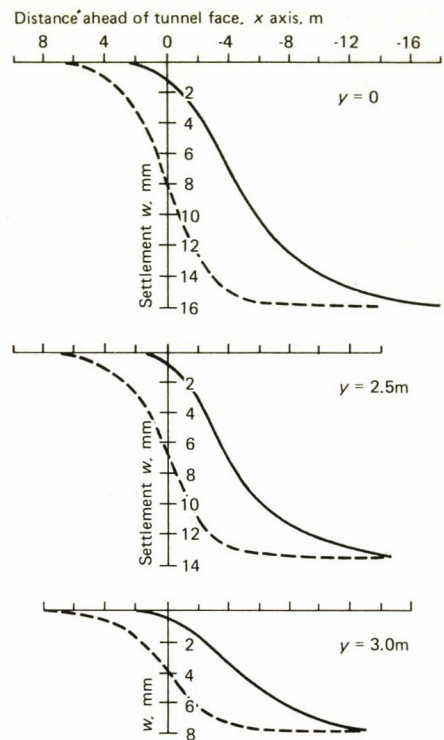


Fig. 6. Forward x-coordinate settlement development profiles for a tunnel in Belfast sleech (Glossop & Farmer, 1977). Full line is measured profile; broken line is theoretical profile (50% w_{\max} assumed coincident with plane of tunnel face)

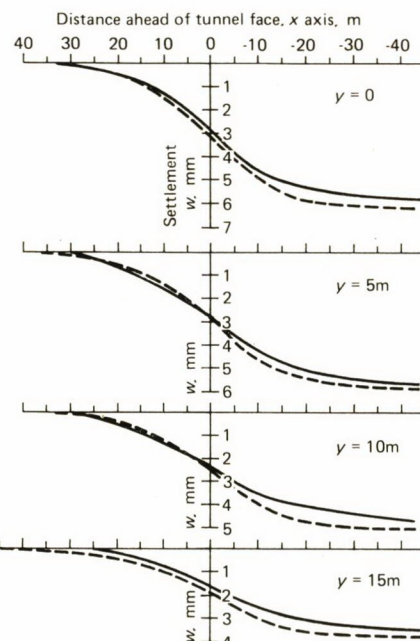


Fig. 5. Forward x-coordinate settlement development profiles for a Jubilee Line running tunnel at Green Park Station, London in London Clay (see Attewell & Farmer, 1974). Full line is measured profile; broken line is theoretical profile (50% w_{\max} assumed coincident with plane of tunnel face)

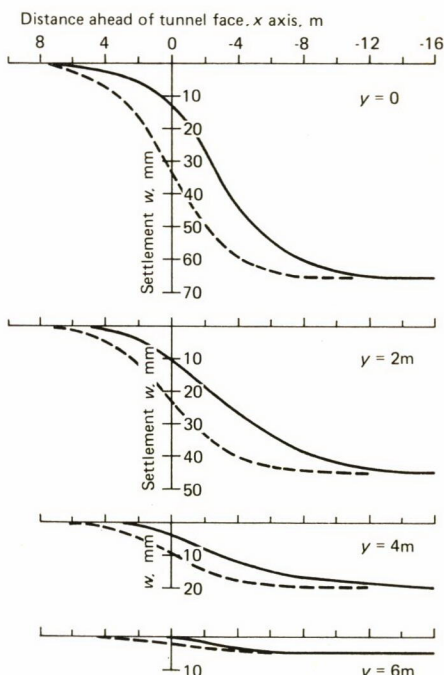


Fig. 7. Forward x-coordinate settlement development profiles for a tunnel at Grimsby in alluvial silt (Glossop, 1980). Full line is measured profile; broken line is theoretical profile (50% w_{\max} assumed coincident with plane of tunnel face)

are taking place) it would seem, from an examination of the several predicted and measured curves, that a better match could be achieved by assigning local ground loss sub-maxima to different positions at and back from the tunnel face. As a general design guide for tunnelling in, for example, firm-to-stiff clay, the ratio w/w_{\max} at $x = 0$ (the face position) would

seem to lie between 30 and 50% with an average value at about 40%. Contributing to this percentage will be a portion of the losses at the face plus a decreasing portion of the losses back down the shield and the lined tunnel. It will also be noted that the losses at the face contribute substantially to the settlement projected beyond the face ($x > 0$). In such a clay,

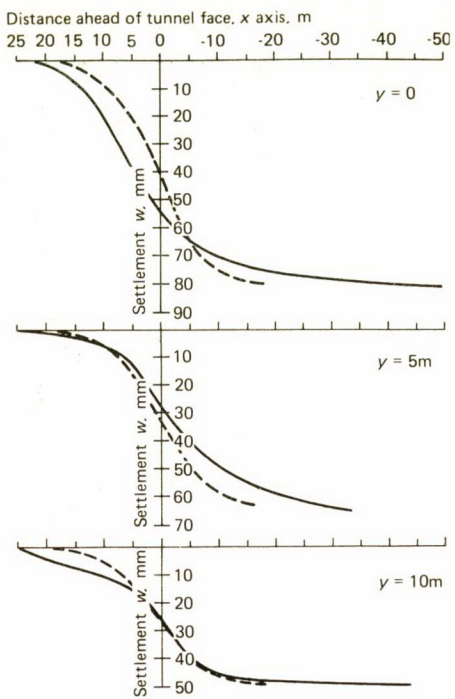


Fig. 8. Forward x-coordinate settlement development profiles for Northumbrian Water Authority's Contract 276 (Ouseburn) North Bank Interceptor Sewer in filled ground (see Dobson *et al.*, 1979). Full line is measured profile; broken line is theoretical profile (50% w_{\max} assumed coincident with plane of tunnel face)

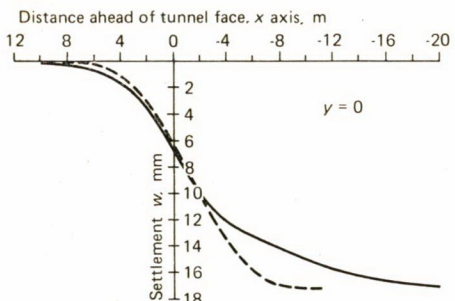


Fig. 9. Forward x-coordinate centre line settlement development profile from a sewer tunnel in Newcastle upon Tyne. Construction at the point of measurement was partly in clay and partly in fill, with fill overburden. Full line is measured profile; broken line is theoretical profile (50% w_{\max} assumed coincident with plane of tunnel face)

practical observation suggests that discernible settlement development would extend over a distance of approximately $1z_0$ ahead of, and $2z_0$ behind the tunnel face. This attenuated settlement behind the tunnel face can be modelled by assigning, say, a ground loss of 80% to the face, and the remaining 20% to the point $x = -z_0$. If the face advanced at a uniform rate, then, given the means to perform calculations rapidly, the total loss can be distributed along the tunnel to match an x-axis settlement profile. It is pointed out that the form of the x-axis profile over a distance $x/z_0 \gtrsim -0.25/x/z_0$ (that is, the forward profile and the advance portion of the lagging profile) is relatively insensitive to such distribution of ground loss.

An underlying problem in such predictive analyses is the assignment of a settlement volume figure, and a value for the n -parameter. The latter is determined from the variation of the transverse settle-

ment trough with depth (see Appendix A(iii)). The former depends strongly upon the geotechnical properties of the ground at and above tunnel level. Both parameters are interdependent, and rely, for their application, upon a corpus of case history data. Reference may be made to the data tables in Attewell (1978), and to Norgrove *et al.* (1979), for the selection of n -values, and it is noted that more case history data has become available since those dates. It should also be noted in the equations given earlier that the predicted settlements, displacements, and strains, are directly proportional to the chosen values of settlement volume or maximum settlement, but not to n , and so a sensitivity analysis on these parameters is not straightforward.

4. Example

Assume that it is proposed to tunnel through filled ground, and the ground movements in the vicinity of an in-ground structure 1.5m below ground level are to be examined. Relevant data are listed below:

- Soil: cohesive fill.
- Tunnel depth from ground surface: 9.2m.
- Tunnel depth from in-ground structure: 7.7m.
- Tunnel excavated diameter: 2.44m.
- Predicted settlement volume: 5% of excavated face area.
- Predicted $K = 1$; predicted $n = 1$. (K_a is independent of a when $n = 1$, and so $K_a \equiv K$).
- Inflexion distance i : 3.85m (from c and f — see equation in Section 2 introduction).

From eqn. 14, Fig. 10a may be constructed. Additionally or alternatively, plan settlement contours may be constructed around the tunnel face. The predicted maximum settlement ($y = 0$) is 24.23mm (Fig. 10a), and the $0.5w_{\max}$ point is located, for convenience, on the graph at $x = 0$. For practical assessment it would be recommended that the $x = 0$ ordinate axis be re-set to intersect the cumulative probability curve ($y = 0$) at $w = 9.7\text{mm}$ (i.e. $0.4w_{\max}$), this re-set applying for all y .

Predicted x-coordinate strains and displacements are shown in Figs. 10b and 10c, respectively and, as with the settlements, could be presented as plan contour plots. As above, an x-axis re-set forward for $x = 0$ at $x = 1.1\text{m}$ would be appropriate.

Predicted y-coordinate strains and displacements are shown in Figs. 10d and 10e, respectively, and again these could be presented as plan contour plots. A re-set of the $x = 0$ axis would require each curve to be relabelled for its specified x distance minus 1.1m.

5. Conclusions

By assuming that the soil at ground surface undergoes no volume change, and that ground movement is the sum total of elementary movements of assumed form resulting from increments of tunnel advance, it is possible to derive expressions which quantify the soil movement ahead and at the sides of a tunnel face. With empirical support and some theoretical justification, these expressions are based on a normal probability form of transverse settlement trough, and a cumulative probability form of centre line trough. The primary expressions for ground loss settlements

seem to approximate fairly well to measured settlement profiles on and parallel to the tunnel centre line. The greatest departure from the predicted form occurs at the fully-developed end of the centre-line profile, and an explanation for this has been suggested in terms of a distribution of ground loss along the tunnel, and a consolidation settlement contribution.

Although ground surface settlement can be measured relatively easily by precise levelling, lateral movements and strains, being smaller in magnitude, can be measured only with great difficulty, if at all. Analytically, because of the relative insensitivity of the integration operation to the assumed form of the transverse settlement curve, a higher degree of reliance may be placed on the equations for ground displacement than on those for ground strain, gradient and curvature which involve differentiations of the profile equation. Furthermore, the results should be seen as pertaining to an approximate general model, which may not apply very well to any particular case, both because of the assumptions made and the local variations on site.

More three-dimensional deformation data are needed from field measurements in order to provide a basis for modifying and extending the above approach, which can perhaps be justified at the present time mainly on the grounds of convenience. In the longer term a physical understanding of the ground deformation mechanisms, perhaps on the lines discussed by Atkinson & Mair (1981), should prove to be more rewarding, and may go some way towards answering the criticisms of de Mello (1981). In both the short and long terms, a major objective must be to interpret the predicted ground movements in terms of above-ground and in-ground structural response.

Acknowledgements

Mr. R. McMillan and Mr. J. Yeates provided much of the encouragement for pursuing the analyses in the Paper and offered valued comments on an earlier draft. The authors are grateful for the interest shown.

Dr. I. W. Farmer and Dr. N. H. Glossop of Newcastle upon Tyne University kindly provided the case history information on the Belfast and Grimsby tunnels.

Some of the preliminary work was performed by Mr. R. I. G. Gordon as part of his MSc. Engineering Geology Advanced Course at Durham University.

References

- Atkinson, J. H. & Mair, R. J. (1981): "Soil mechanics aspects of soft ground tunnelling", *Ground Engineering*, v. 14, No. 5, pp. 20-26.
- Attewell, P. B. (1978): "Ground movements caused by tunnelling in soil", *Proc. Conf. on Large Ground Movements and Structures*, Cardiff, July 1977, Ed. Geddes, J. D., Publ. Pentech Press, London, pp. 812-948.
- Attewell, P. B., Farmer, I. W. & Glossop, N. H. (1978): "Ground deformation caused by tunnelling in a silty alluvial clay", *Ground Engineering*, v. 11, No. 8, pp. 23-41.
- Attewell, P. B. & Farmer, I. W. (1974): "Ground disturbance caused by shield tunnelling in a stiff overconsolidated clay", *Engineering Geology*, v. 8, pp. 361-381.
- Attewell, P. B., Farmer, I. W., Glossop, N. H. & Kuszniar, N. J. (1975): "A case history of ground movement by tunnelling in laminated clay", *Proc. Conf. on Subway Construction*, Budapest-Balatonfüred, pp. 165-178.
- Attewell, P. B. & Farmer, I. W. (1973): "Measurement and interpretation of ground movements during construction of a tunnel in laminated clay at Hebburn, County Durham", Report to Transport and Road Research Laboratory, DoE, Research Contract No. ES/GW/842/68.
- Craig, R. (1975): "Discussion at meeting of British Tunnelling Society, *Tunnels and Tunnelling*", v. 7, pp. 61-65.